Dynamic Support Interference

J. PETER READING* AND LARS E. ERICSSON†
Lockheed Missiles Space Company, Sunnyvale, Calif.

Available experimental results are reviewed and organized to provide a logical explanation of aerodynamic support interference for dynamic wind-tunnel testing. Configurations involving bulbous bases, mass addition, boundary-layer transition near the base, and hypersonic low-density flows are shown to be particularly sensitive to sting interference effects. Transverse rod support interference occurs at all Mach numbers depending on oscillation amplitude and/or trim angle of attack. The postulated flow model predicts that cylindrical and flared stings can have opposite interference effects in agreement with experimental observations. An analytical method of correcting the wind-tunnel results for dynamic support interference is proposed.

Nomenclature

c = reference length (maximum diameter)
d_s = sting diameter
L_s = sting length
M = Mach number
m = pitching moment coefficient $C_m = m/(\rho_\infty V_\infty{}^2/2)Sc$
N = normal force coefficient $C_N = N/(\rho_\infty U_\infty{}^2/2)S$
q = pitch rate
r = radius
r_b = base radius
S = reference area ($S = \pi c^2/4$)
t = time
U = velocity
w = upwash velocity
x,z = horizontal and vertical coordinates ($c\xi$ and $c\zeta$, respectively)
α = mean angle of attack
$\Delta\alpha$ = amplitude of pitch oscillation
δ = sting deflection
Δ = difference
θ = pitch attitude
ω = pitch frequency

Subscripts

d = downstream communication through boundary layer
I = total interference
R = transverse rod interference
S = separation location
u = boundary-layer upstream communication
w = wake neck or wake upstream communication
1 = within wake separation
2 = upstream of wake separation

Superscripts

i = induced, e.g., $\Delta^i C_N$ = separation induced normal force coefficient

Differential Symbols

$\dot{\alpha} = \partial\alpha/\partial t$
$C_{m_\alpha} = \partial C_m/\partial\alpha$
$C_{m_{\dot{\alpha}}} = \partial C_m/\partial(\dot{\alpha}c/U)$
$C_{m_q} = \partial C_m/\partial(cq/U)$
$C_{m_{\dot{q}}} = \partial C_m/\partial(c^2\dot{q}/U^2)$
$C_{m_\delta} = \partial C_m/\partial\delta$
$\dot{z} = \partial z/\partial t$

Presented as Paper 71-277 at the AIAA 6th Aerodynamic Testing Conference, Albuquerque, N. Mex., March 10–12, 1971, submitted September 22, 1971; revision received February 24, 1972. This work is the result of a study of the dynamics of bulbous based bodies conducted for the NASA Langley Research Center under the direction of H. G. Wiley (Contract NAS 1-6450).

Index categories: Re-Entry Vehicle Testing; Nonsteady Aerodynamics; Jets, Wakes, and Viscid-Inviscid Flow Interactions.

* Research Specialist. Member AIAA.
† Senior Staff Engineer. Associate Fellow AIAA.

Introduction

SUPPORT interference has always been of great concern in wind-tunnel testing. Dynamic test results are particularly sensitive to the support system configuration since both elastic and aerodynamic coupling with the model-balance system can occur. Much of the evidence regarding aerodynamic support interference is confusing and sometimes appears contradictory. For instance, the slender, bulbous based body in Fig. 1[1] definitely experiences support interference; also Wehrend's results show that the sting can cause interference on bulbous based bodies.[2] Likewise, at higher amplitudes the transverse rod can affect the forebody damping. At precisely what amplitude the transverse rod begins to affect the damping and how this is modified by the bulbous base is unknown. Furthermore, Wehrend has also shown that cylindrical and flared stings can have similar interference effects (compare Figs. 2 and 3). Walchner and Clay have observed the opposite effect of a sting-flare at hypersonic speeds for a flat based cone.[3] Transverse rod interference is also present at hypersonic speeds (compare Figs. 12 and 13 in the text),[1,4] which is no surprise; but why should a flat based cone at hypersonic speeds experience sting interference effects similar to those of a bulbous based cone at transonic speeds? The flow model proposed herein attempts to answer these and other questions concerning dynamic support interference and proposes a means of correcting the experimental results for these unwanted effects.

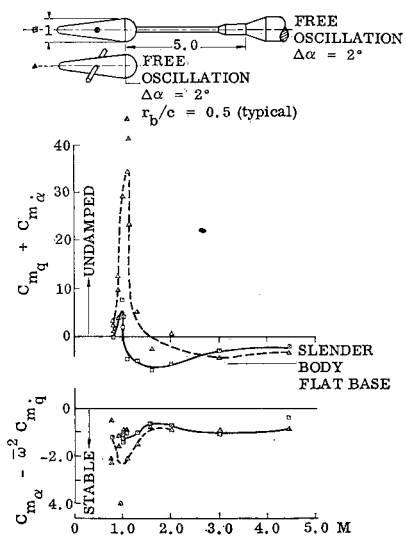

Fig. 1 Dynamic support interference on a hemispherical based slender cone.

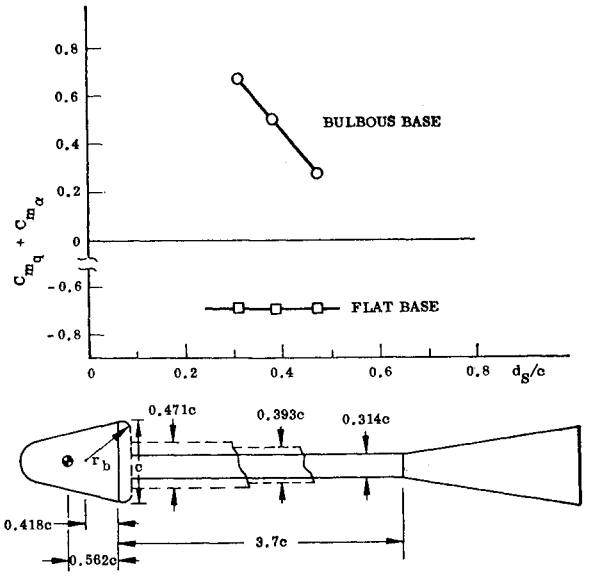

Fig. 2 Effect of sting size on the damping of a bulbous based body, $M = 0.65$.

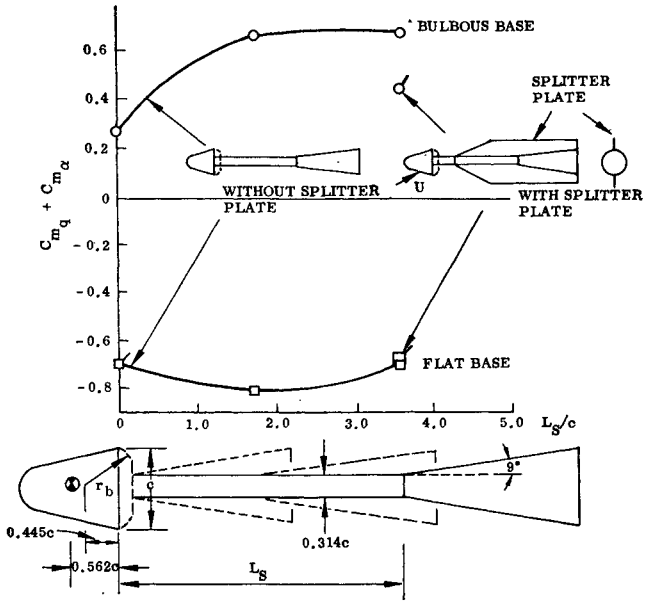

Fig. 3 Effect of sting flare on the damping of a bulbous based body, $M = 0.65$.

Flow Models

It has been shown that the interaction between the near wake and a bulbous base causes dynamic instability.[5] Certainly, then, the presence of a sting must affect the dynamic stability. In fact, this is what Wehrend was investigating when he obtained his telling sting interference data of Figs. 2 and 3.[2] Just how much of these unusual bulbous base effects are due to sting interference, is difficult to ascertain. However, free-flight results have amply demonstrated that the bulbous base causes a nonlinear undamping effect (Fig. 4).[6] This undamping effect is the result of unequal windward and leeward side wake neck pressures that are convected upstream through the wake recirculation to perturb the wake separation point. The unequal wake neck pressures (higher on the windward side) are the result of the transverse pressure gradient imposed by the freestream in turning the inclined wake parallel to the freestream. These wake effects are opposed

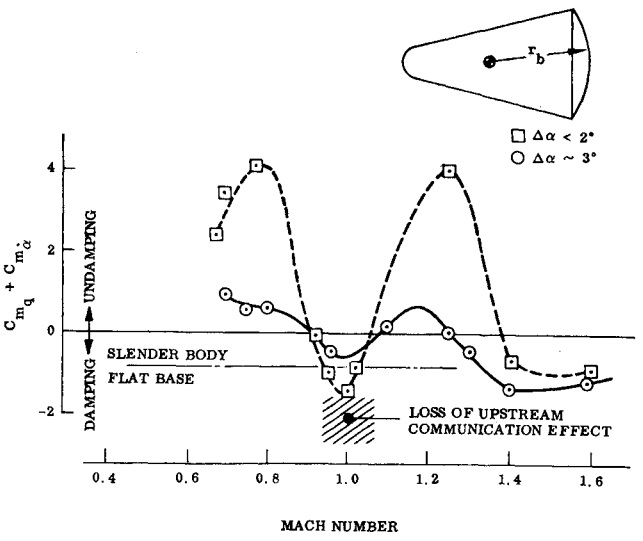

Fig. 4 Free-flight damping of a bulbous based cone.

by the tendency of the leeward boundary layer, thickened by forebody crossflow effects, to cause the leeward separation point to move forward. That the near wake effects tend to dominate may be seen in Fig. 5.‡

Of course, the dominance of the wake effect depends upon the strength of the pressure rise at the separation point relative to the wake neck. When a terminal normal shock occurs at the wake separation point the pressure rise there is much larger than at the wake neck, and the near wake effects vanish (Fig. 4). A sting, of course, alters the wake geometry and enhances the wake neck pressure differential, since the sting can support a greater pressure gradient than can a free wake.

Dynamic Sting Interference

Dynamic sting interference is quite different from the static variety since in the usual dynamic test set-up the model pitches relative to the sting (rather than the two pitching together). Thus, the dynamic interference load will be negative or statically destabilizing. (Compare Figs. 6a and 6b.) When the rotation center is forward of the base, base plunging effects further aggravate the sting interference.

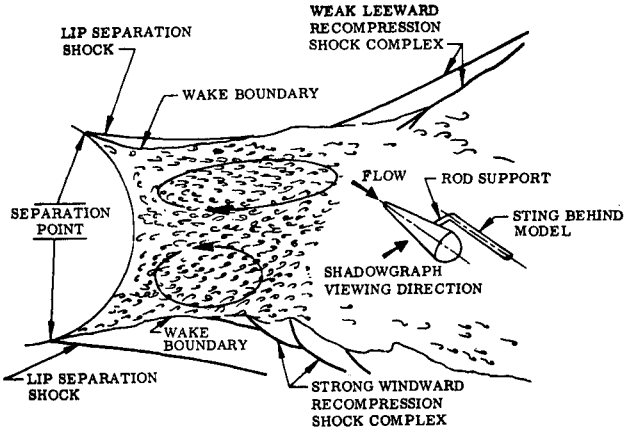

Fig. 5 Near wake flow pattern of a slender cone with rounded base, $M = 2.0$, $\alpha = 12°$.

‡ The wake of the transverse rod on the back side of the model serves to further enhance the boundary-layer effect by adding to the viscous layer. Therefore, the separation would be even more asymmetric in the free-flight case.

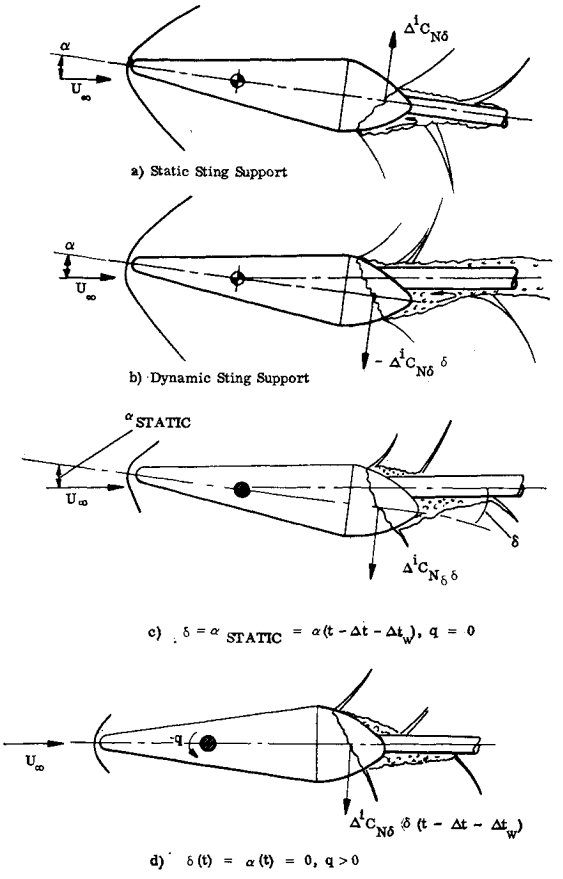

Fig. 6 Steady and unsteady cylindrical sting induced base load.

In the unsteady case the interference load lags the vehicle motion due to the finite convection speed downstream to the wake neck and the following upstream convection through the wake recirculation region. Thus, a residual interference load occurs (as the body pitches downward through $\alpha = 0$) which opposes the motion (compare Figs. 6c and 6d). Thus, the interference effect of a cylindrical sting is damping (but statically destabilizing).

The wake recirculation region plays a similar role in flared sting interference, except that the flare may cause an opposite interference load. When a cone is pitched in the wake neck it introduces an upwash in the wake recirculation region which expands the leeward wake and, if the wake separation point is free to move, the wake source base load will be affected (as for the asymmetric flared sting in Fig. 7). A similar crossflow phenomenon is evident in the recirculation region for nose-induced separation (Fig. 8),[7] and has been shown to be responsible for dynamic instability of conic decelerators.[8]

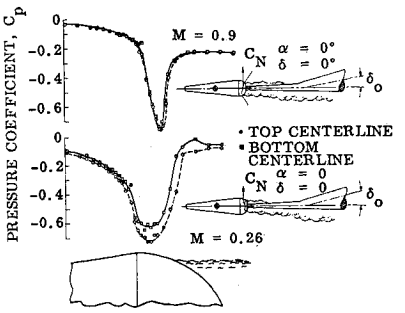

Fig. 7 Pressures on a hemispherical base with flared sting interference.

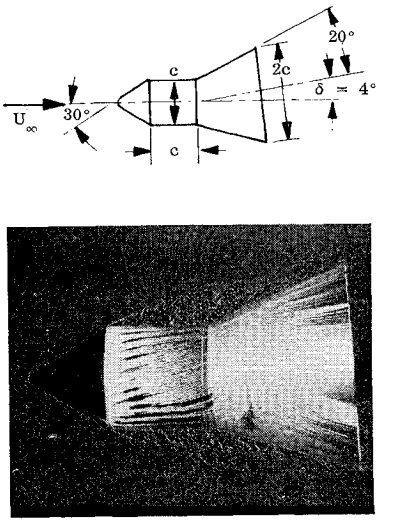

Fig. 8 Crossflow patterns in the recirculation region for nose induced separation.

Results for wake submerged cones show that the sign of the interference load reverses for very short separation distances.[8] This occurs when the tendency of the higher windward side recompression pressure to expand the windward wake dominates the crossflow effect in the recirculation region. Thus, moving the sting flare forward to the model base reduces the undamping effect of the flared sting (Fig. 3). The asymmetrically flared sting in Fig. 7 generates a statically stabilizing interference load due to the effective sting deflection δ_0. The correlation between dynamic stability, static stability, and sting deflection derivative measured by Adcock[9] shows conclusively that the flared sting produces an undamping (and statically stabilizing) interference effect (Fig. 9).§

The interference load is not necessarily restricted to the bulbous base. A rounded base shoulder seems to facilitate the modification of the aft body loading. The loads directly on the bulbous base itself cannot be responsible for the undamped free-flight results shown in Fig. 4. It has been shown that when transition occurs near the base at transonic speeds,

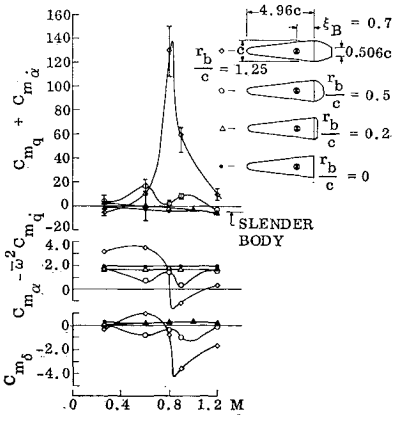

Fig. 9 Correlation of static and dynamic flared sting results for bulbous based bodies.

§ The support interference derivative reaches its maximum when the sting flare is centered in the wake neck ($\delta_0 = 0$). In this case the wake is unstable at $\delta_0 = 0$ resulting in discontinuous interference characteristics.[1] Flowfield hysteresis precluded traversing the discontinuity for the small oscillation amplitude used ($\Delta\alpha = 1°$); thus, the maximum interference effect was not realized.

a flat based cone can also be affected by dynamic sting interference.[10] The sensitivity of transition location to adverse pressure gradient provides the mechanism whereby the wake (perturbed by the sting) affects the loads forward of the base and thereby the damping. Whenever there is a flow mechanism through which the wake can affect the loads forward of the base, sting interference results. The thick laminar boundary layer existing in ground tests at hypersonic speeds provides such a flow mechanism. The presence of the sting affects the lip shock strength via the wake neck recompression and the near wake recirculation regions. This pressure change is propagated upstream of the base to an extent that is roughly proportional to the boundary-layer thickness.[11] At high Mach numbers and very low Reynolds numbers the lip and wake-neck shocks appear to merge[11] allowing the sting to affect the lip shock almost directly. This explains the flared sting interference effects measured by Walchner and Clay (Fig. 10).[3] The nonlinear damping results of Hobbs (Fig. 11),[4] which bear such a similarity to the bulbous base results, also appear to be due to interference effects from an asymmetric sting flare.[12]

Any attempt to simulate ablation, either by using low-temperature ablators or gas injection, increases the probability of dynamic sting interference. Not only is the extent of any upstream effect of base influence enhanced by the thicker boundary layer, but the coalescence of lip and wake neck shocks is promoted. When gas injection or blowing is used to simulate ablation, the sting is usually large to accommodate the necessary plumbing, further increasing the potential for dynamic sting interference.

Transverse Rod Interference

One obvious way to avoid the problem of dynamic sting interference is to use a transverse rod support. However, it has been amply demonstrated that a transverse rod,[13] or a wire support located near the wake separation point,[14] can have a profound effect on the wake geometry. Obviously this will invalidate the damping measurements of bulbous based bodies since the unperturbed wake effect adds an important contribution to the damping. However, it may not be too serious for flat based configurations.

Of course, rod positions forward of the base are of greater practical interest since few (if any) flight vehicles have a center of gravity at the base. At transonic speeds it appears that even this rod interference is not a serious problem for low

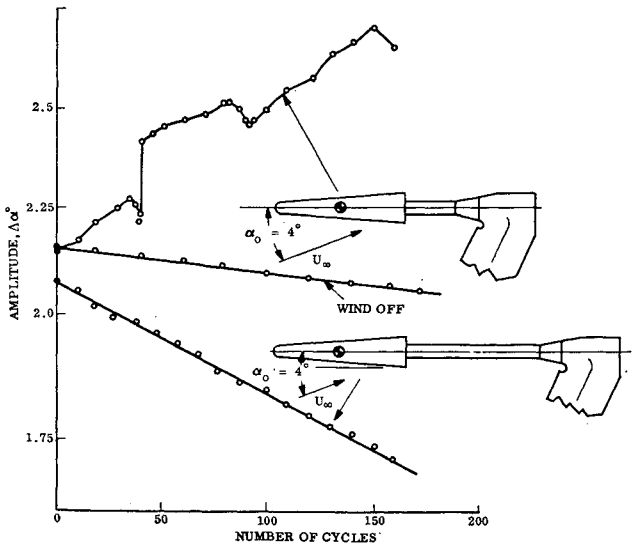

Fig. 10 Effect of sting flare on the dynamics of a slender cone, $M = 14$.

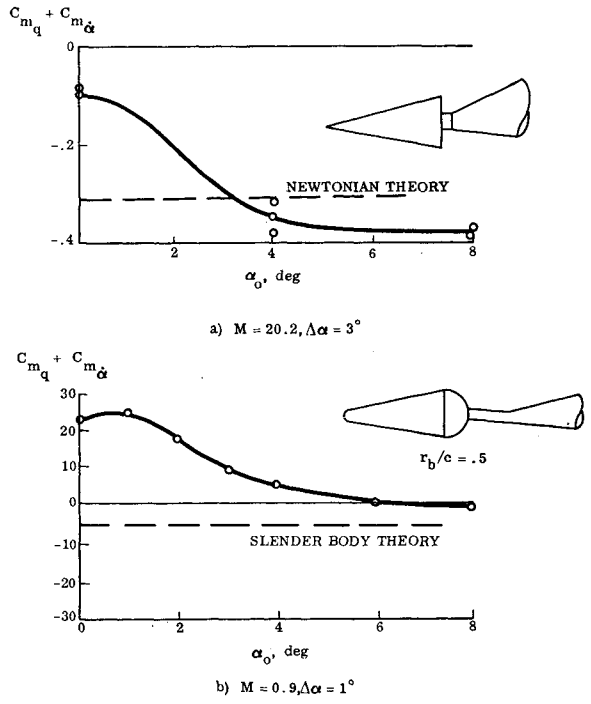

Fig. 11 Comparison of hypersonic and transonic flared sting interference.

amplitudes and/or trim angles (Fig. 12).¶ However, at hypersonic speeds appreciable rod interference is realized even for low-amplitude oscillations about zero angle of attack (Fig. 13). In both cases the interference effect is undamping. As in the case of sting interference, the static and dynamic effects of rod interference are opposite (Fig. 12), indicating the presence of a flowfield time lag. The increased static stability is due to reduced leeward side dynamic pressure as the rod wake sweeps over the aft body

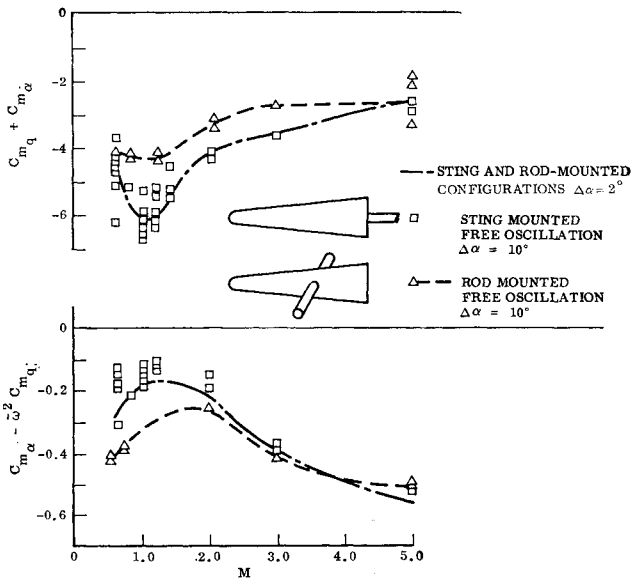

Fig. 12 Transverse rod interference.

¶ Because rod and sting results agree at low amplitude ($\Delta\alpha = 2°$) one may assume interference effects are absent. Likewise, since the sting mounted results at $\Delta\alpha = 10°$ agree with the $\Delta\alpha = 2°$ results, one may further assume sting interference effects are also absent for the flat based, slender cone with its linear aerodynamics.

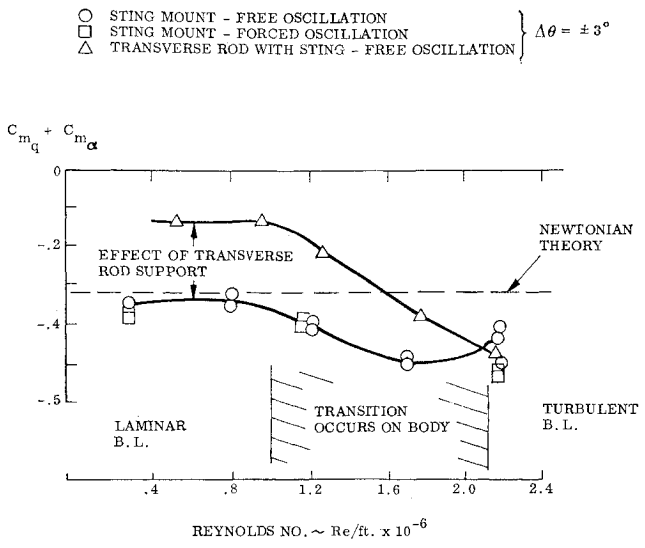

Fig. 13 Transverse rod interference, $M = 10$.

at angle of attack. The rod wake does not trail directly behind the rod, but is swept upward as the result of the increased crossflow at the lateral meridians. Inviscidly the crossflow at the lateral meridians is approximately double the freestream angle of attack. The viscous streamlines tend to turn even more, so that local crossflow angles at the body-rod juncture of three to four times the freestream angle of attack are not unusual.[15]

In the unsteady case, the additional wake angle $\tan^{-1} \Delta w/U_\infty$ (Fig. 14) lags the body motion due to the finite convection speed in the rod wake; thus, the induced force $\Delta^i C_N$ will lag the body motion, and the statically stabilizing tail load is dynamically destabilizing or undamping. At small values of $\Delta w/U_\infty$ the wake will be restricted to the lateral meridians, thus having negligible effect on longitudinal characteristics. When the ratio $\Delta w/U_\infty$ increases, as with the increased viscous effects at hypersonic speed, rod interference becomes appreciable already at low angles of attack (compare Figs. 12 and 13).

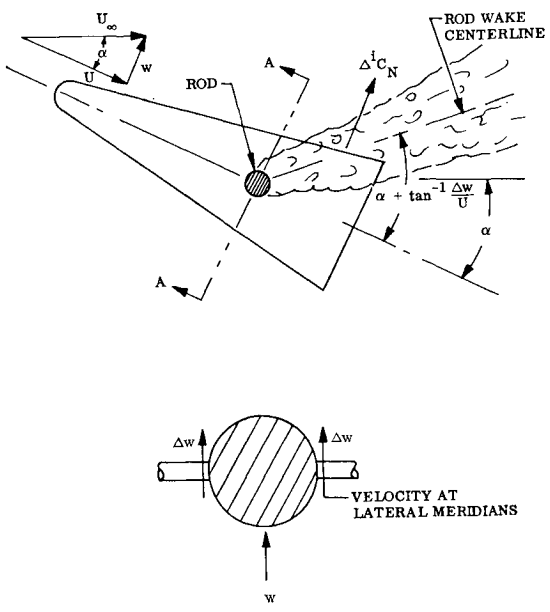

Fig. 14 Rod wake interference at large angles of attack.

Elimination of Support Interference

The proposed flow models explain the observed interference effects; however, they do not define quantitatively at what flow conditions and for what configurations one might expect support interference. Free-flight techniques obviously avoid sting interference. However, it is often desirable to be able to achieve the more controlled conditions of a wind tunnel test. Thus, it would be useful to have some means of correcting wind-tunnel data for interference effects.

Quasi-Steady Technique

Wake flow theories are not sufficiently advanced to produce a means for correcting wind tunnel measurements for support interference. However, it appears possible to achieve such ends by combining static experimental data with quasi-steady analytical techniques. This approach has had considerable success in the past.[16,17]

In classical quasi-steady theory the force is defined as

$$C_{Nqs} = C_N\alpha_0 + C_{N_2}\tilde{\alpha} \tag{1}$$

where

$$\tilde{\alpha} = \theta + \dot{z}/U$$

This formulation is valid for aerodynamic forces that depend only on the instantaneous local angle of attack. However, the support interference load is primarily a function of flow conditions elsewhere, e.g., at the wake neck. The interference loads can be expressed as follows:

$$\Delta^i C_{Nqs}(t) = \Delta^i C_N(\alpha_0) + \Delta^i C_{N_2}\tilde{\alpha}(t - \Delta t) \tag{2}$$

That is, the induced interference load at time t is determined by the generalized angle of attack at the earlier time, $t - \Delta t$. In the case of the sting support it is assumed that the sting deflection loads will be available from special static results similar to those obtained by Adcock (Fig. 9).[9] Consider the model with a cylindrical sting (Fig. 15).** The interference load may be represented by two lumped loads, one upstream and one downstream of the wake separation point,

$$\Delta^i C_{N\delta} = \Delta^i C_{N\delta 1} + \Delta^i C_{N\delta 2} \tag{3}$$

The quasi-steady cylindrical sting load is

$$\Delta^i C_{Nc}(t) = \Delta^i C_{N1}(\alpha_0) + \Delta^i C_{N2}(\alpha_0) + \Delta^i C_{N\delta 1}\tilde{\alpha}_1(t - \Delta t_1) + \Delta^i C_{N\delta 2}\tilde{\alpha}_2(t - \Delta t_2) \tag{4}$$

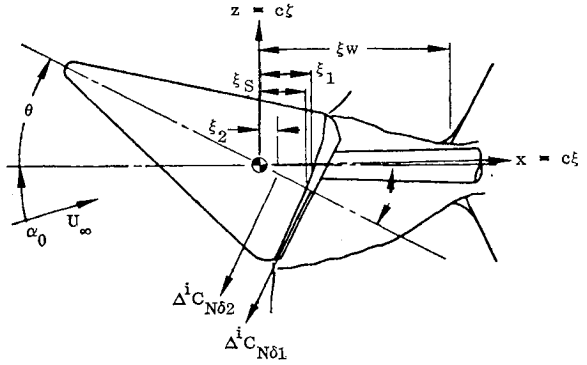

Fig. 15 Sting interference.

** The angles α_0, θ, and δ are small (they are exaggerated in Fig. 15).

where

$$\tilde{\alpha}_1 = \theta + \xi_1 c\dot{\theta}/U_\infty, \qquad \tilde{\alpha}_2 = \theta + \xi_2 c\dot{\theta}/U_\infty,$$
$$\Delta t_1 = (U_\infty/\bar{U}_d + U_\infty/\bar{U}_w)(\xi_w - \xi_s)\, c/U_\infty$$
$$\Delta t_2 = \Delta t_1 + (U_\infty/\bar{U}_u)(\xi_s - \xi_2\, c/U_\infty,$$

$\bar{U}_d$ = downstream wake communication velocity

$\bar{U}_w$ = upstream wake communication velocity

$\bar{U}_u$ = upstream communication velocity in the boundary layer

For slow oscillations, $(\omega c/U_\infty)^2 \ll 1, \tilde{\alpha}(t - \Delta t)$ can be approximated as follows:

$$\tilde{\alpha}(t - \Delta t) = \theta(t) - \Delta t\dot{\theta}(t) + \xi c\dot{\theta}(t)/U_\infty \tag{5}$$

Substituting Eq. (5) into Eq. (4) and taking $\partial/\partial(\dot{\theta}c/U_\infty)$ gives the unsteady interference load, where $\delta = \tilde{\alpha}$.

$$\partial\Delta^i C_{N\delta}/\partial(\dot{\theta}c/U_\infty) = -$$
$$(\Delta^i C_{N\delta 1} + \Delta^i C_{N\delta 2})(U_\infty/\bar{U}_d + \bar{U}_\infty/\bar{U}_w)(\xi_w - \xi_s) +$$
$$\Delta^i C_{N\delta 1}\,\xi_1 - \Delta^i C_{N\delta 2}[(U_\infty/\bar{U}_u)(\xi_s - \xi_2) - \xi_2] \tag{6}$$

The moment derivative is simply obtained by $\Delta^i C_{m\delta} = -\xi\Delta^i C_{N\delta}$. The unsteady interference moment derivative can be subtracted from the measured damping derivative $(C_{m\dot{\theta}})_m$ to give the corrected damping derivative $C_{m\dot{\theta}}$.

$$C_{m\dot{\theta}} = (C_{m\dot{\theta}})_m - \partial\Delta^i C_{m\delta c}/\partial(\dot{\theta}c/U_\infty) \tag{7}$$

A similar procedure may be followed to obtain the flared sting interference effect.

Actually, the bulk of the interference load is the result of base plunging; thus, the measured interference load is

$$\Delta^i C_{N\delta} = \partial(\Delta^i C_N)/\partial\delta + [\partial(\Delta^i C_N)/\partial\zeta](\partial\zeta/\partial\delta) \tag{8}$$

Furthermore, if the interference load is obtained from static force measurements, one does not usually know both upstream and downstream components separately, but only the total interference load $\Delta^i C_{N\delta I} = \Delta^i C_{N\delta 1} + \Delta^i C_{N\delta 2}$. Thus, the unsteady interference load is

$$\partial\Delta^i C_{N\delta}/\partial(\dot{\theta}c/\bar{U}_\infty) = -$$
$$\Delta^i C_{N\delta I}[(U_\infty/\bar{U}_d + U_\infty/\bar{U}_w)(\xi_w - \xi_I) - \xi_I] \tag{9}$$

ξ_I is substituted for ξ_1 and ξ_2, where $\xi_I = \xi_s$ is the assumed center of pressure for the total interference load.

The rod interference effect can be derived in a similar manner. The sweeping of the wake to the leeward side depends on the crossflow at the rod location which in turn can be related to the angle of attack. Thus, from Fig. 16

$$\zeta_R(t) = [\partial\zeta_R/\partial\alpha]\,[\partial\alpha_R/\partial\alpha]\,\tilde{\alpha}(t - \Delta t) \tag{10}$$

where $\tilde{\alpha} = \alpha_0 + \theta$ ($\dot{z} = 0$ at the rotation center) and $\Delta t_R = (U_\infty/\bar{U}_R)(\xi_R c/U_\infty)$.

The induced load due to the reduction of the leeward side dynamic pressure within the rod wake is

$$\Delta^i C_{N\alpha R} = (\Delta\bar{q}/q_\infty)\, C_{\bar{p}}\,(\partial S_R/\partial\zeta_R)\,(\partial\zeta_R/\partial\alpha) \tag{11}$$

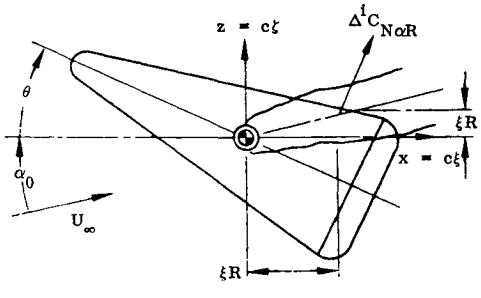

Fig. 16 Rod interference.

where $\Delta\bar{q}$ is the average reduction in the wake dynamic pressure; $C_{\bar{p}}$ is the average attached flow pressure coefficient in the area covered by the rod wake, and S_R is the normal projection of the area within the rod wake.

If static measurements are used, $\Delta^i C_{N\alpha R}$ is measured directly. Following the same steps as for the sting interference load yields

$$\partial\Delta^i C_{NR}/\partial(\dot{\theta}c/U_\infty) = -\Delta^i C_{N\alpha R}(U_\infty/\bar{U}_R)\xi_R \tag{12}$$

which may be multiplied by $-\xi_R$ and the result subtracted from $(C_{m\dot{\theta}})_m$ to give the corrected damping.

The alteration of the basic wake geometry by the presence of the sting has been neglected. Certainly, a sting will change the location of the wake separation point even at $\alpha = 0$ which will affect the loads and therefore the damping. Similarly, the rod wake will interact with the body wake and affect the loads.

By neglecting these effects we have assumed that the support system is small. In addition to the interference loads the communication speeds (U_d, $\bar{U}_w$, and $\bar{U}_R$) must be known. They can be determined by correlating unsteady pressure measurements within the wake or by measuring wake velocity profiles. Both involve difficult experimental techniques. However, the use of free wake communication velocities is consistent with the assumption of a small support system. Adcock's data[9] were corrected in this manner by assuming a small support system (Fig. 17).

It is unfortunate that no interference free data are available for comparing with these results. This points out the need for more definitive experimental data. Not only is there a scarcity of interference free results but, as far as the authors know, there have been no systematic investigations of dynamic sting interference that can define quantitatively where support interference becomes a problem. Likewise, more theoretical work aimed at defining the wake induced loads and their associated time lags would not only make possible correction of wind-tunnel result for support interference but would also provide better estimation of the flight vehicle characteristics.

Other Approaches

It may be possible in many instances to use experimental results to extrapolate to zero sting size. The difficulty with this approach is getting a point sufficiently close to zero sting size while maintaining the necessary sting stiffness. Using a splitter plate or web to stiffen a minimum size sting may add additional interference effects. The mixing of the wake with the splitter plate boundary layer may alter the wake recompression sufficiently to preclude simulation of the free wake. This is also a problem with the half model technique.[18] Wehrend's result indicate that the splitter plate certainly alters the aerodynamic sting interference (Fig. 4).††[2] In any event,

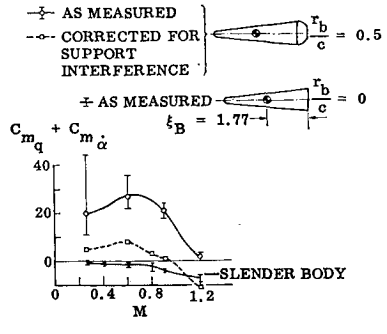

Fig. 17 Damping of a hemispherical based body corrected for sting interference.

†† This is not a case of the splitter plate affecting the sting response or "elastic interference" since there is no effect on the flat based model.

the validity of extrapolating to zero sting size will need to be verified.‡‡ Thus, any definitive study of support interference must involve both wind tunnel and free-flight facilities.

It would be convenient if one could resort to free-flight techniques completely. However, it is often desirable to maintain the more controlled conditions of a wind-tunnel test. In the ballistic range pitch amplitude variations may be modified by nonlinear Mach number effects. The free-flight tunnel may circumvent this problem, but one is still constrained to the use of statically stable models, and it is difficult to achieve nonzero trim angles of attack.[19] Magnetic suspension combines the best of free-flight techniques and wind-tunnel testing, but it is still a long way from being a routine testing tool.

Until such time as the ground rules for avoiding dynamic support interference are better defined, it might be advisable, for sensitive configurations, to test a few sting sizes, as Wehrend did,[2] to determine if there is a problem. This must be done dynamically since the dynamic stability may be significantly affected while the effects on static stability are negligible. In fact, this may always be a good approach, since apparently unconnected configuration changes may alter the support interference. For instance, Olmstead's results[20] indicate that when boundary-layer transition occurs in the wake of a model with a concave base an undamping, statically stabilizing interference effect occurs. Likewise, the measured dynamic effect of boundary-layer transition may be affected by sting interference effects on the concave base.[21,22] A blunt nose, in addition to eliminating the accelerated flow effect,[22] may change the sting interference as well. Peterson and Bogdonoff have shown that nose bluntness has an effect on the hypersonic base pressure by changing conditions forward of the corner.[23] Thus, one wonders how much of the measured effects of nose bluntness are in reaility due to sting interference effects via this nose-near wake coupling.

Conclusion

Dynamic support interference is very much a fact. The presented results show that upstream effects from the near wake region are responsible for the dynamic sting interference. Any configuration that allows base effects to be communicated forward and effect the longitudinal loads will be subject to dynamic sting interference. Transverse rod interference occurs at all speeds at certain trim angles of attack and/or pitch amplitudes. It appears that a quasi-steady analytical correction technique for dynamic sting interference is possible if static support interference measurements and valid estimates or measurements of the pertinent convection speeds are available. What is most needed now is a systematic experimental attack on the problem combining data from wind tunnels and free-flight facilities to define ground rules for minimizing or avoiding sting interference. Such ground rules must consider the fact that support interference is coupled with other geometric parameters such as nose bluntness and base shape. In the interim the experimentalist is cautioned to expect these effects and to design his test in such a manner that their presence can be detected.

References

[1] Ericsson, L. E. and Reding, J. P., "Aerodynamic Effects of Bulbous Bases," CR-1339, Aug. 1969, NASA.

[2] Wehrend, W. R. Jr., "An Experimental Evaluation of Aerodynamic Damping Moments of Cones With Different Centers of Rotation," TND-1768, March 1963, NASA.

[3] Walchner, O. and Clay, J. T., private communication, June 3, 1968, Aerospace Research Lab., Air Force Flight Dynamics Lab., Wright-Patterson Air Force Base, Ohio.

[4] Hobbs, R. B., "Hypersonic Dynamic Stability, Part II Conical Body Experimental Programs, "FDL-TDR-64-149, Pt. II, Jan. 1967, Air Force Flight Dynamics Lab., Wright-Patterson Air Force Base, Ohio.

[5] Ericsson, L. E. and Reding, J. P., "Re-Entry Capsule Dynamics," *Journal of Spacecraft and Rockets*, Vol. 8, No. 6, June 1971, pp. 575–586.

[6] MacAllister, L. C., "Some Instability Problems With Re-Entry Shapes," BRL Memo Rept. 1224, Aug. 1959, Ballistics Research Lab., Aberdeen Proving Ground, Md.

[7] Ericsson, L. E., Reding, J. P., and Guenther, R. A., "Analytic Difficulties in Predicting the Dynamic Effects of Separated Flow," *Journal of Spacecraft and Rockets*, Vol. 8, No. 8, Aug. 1971, pp. 872–878.

[8] Reding, J. P. and Ericsson, L. E., "Loads on Bodies in Wakes," *Journal of Spacecraft and Rockets*, Vol. 4, No. 4, April 1967, pp. 511–518.

[9] Adcock, J. B., "Some Experimental Relations Between the Static and Dynamic Stability Characteristics of Sting-Mounted Cones With Bulbous Bases," *Transactions of the 3rd Technical Workshop on Dynamic Stability Problems*, Paper 5, Vol. II, 4–7 Nov., 1968 NASA Ames Research Center, Moffett Field, Calif.

[10] Ericsson, L. E. and Reding, J. P., "Boundary Layer Transition and Dynamic Sting Interference," *AIAA Journal*, Vol. 8, No. 10, Oct. 1970, pp. 1886–1889.

[11] Hama, F. R., "Experimental Studies on the Lip Shock," *AIAA Journal*, Vol. 6, No. 2, Feb. 1968, pp. 212–219.

[12] Hobbs, R. B. Jr., private communication of Sting Geometry, Re-entry Systems Div., 1968, General Electric Co., Valley Forge, Pa.

[13] Reding, J. P., "Partial Simulation of Elastic-Body Dynamics for the Upper-Stage Apollo-Saturn Launch Vehicle," LMSC M-37-67-4, Dec. 1967, Lockheed Missiles & Space Co., Sunnyvale, Calif.

[14] Dayman, B., "Optical Free-Flight Wake Studies," TR 32-364, Nov. 1 1962, Jet Propulsion Lab., Pasadena, Calif.

[15] Rakich, J. V. and Cleary, J. W., "Theoretical and Experimental Study of Supersonic Steady Flow Around Inclined Bodies of Revolution," *AIAA Journal*, Vol. 8, No. 3, March 1970, pp. 511–518.

[16] Ericsson, L. E. and Reding, J. P., "Analysis of Flow Separation Effects on the Dynamics of a Large Space Booster," *Journal of Spacecraft and Rockets*, Vol.2, No. 4, July–Aug. 1965, pp. 481–498.

[17] Ericsson, L. E. and Reding, J. P., "Dynamics of Separated Flow Over Blunt Bodies," LMSC 2-80-65-1, Dec. 1965, Lockheed Missiles and Space Co., Sunnyvale, Calif.

[18] LaBerge, J. G., "Effect of Flare on the Dynamic and Static Moment Characteristics of a Hemisphere-Cylinder Oscillating in Pitch at Mach Numbers from 0.3 to 2.0," LR-295, Jan. 1961, National Research Council of Canada, Ottawa, Ontario, Canada.

[19] Dayman, B. Jr., "Simplified Free-Flight Testing in a Conventional Wind Tunnel," CIT-JPL TR 32-346, California Inst. of Technology, Jet Propulsion Lab., Pasadena, Calif.

[20] Olmstead, G. S., "An Investigation of the Dynamic Stability of a Slender Cone at Supersonic Mach Numbers," *Transactions of the 3rd Technical Workshop on Dynamic Stability Problems*, Vol. IV, Paper 8, Nov. 4–7, 1968, NASA Ames Research Center, Moffett Field, Calif.

[21] Ward, L. K., "Influence of Boundary-Layer Transition on Dynamic Stability at Hypersonic Speeds," *Transactions of the 2nd Workshop on Dynamic Stability Testing*, Arnold Engineering Development Center, Tullahoma, Tenn., Vol. II, Paper 9, April 1965.

[22] Ericsson, L. E., "Effect of Boundary Layer Transition on Vehicle Dynamics," *Journal of Spacecraft and Rockets*, Vol. 4, No. 12, Dec, 1969, pp. 1404–1409.

[23] Peterson, C. W. and Bogdonoff, S. M., "An Experimental Study of Laminar Hypersonic Blunt Cone Wakes," AIAA Paper 69-174, San Francisco, Calif., 1969.

‡‡ As the variation with sting size may be very nonlinear near zero sting diameter.